

# Morphology and composition of nanograde calcium phosphate needle-like crystals formed by simple hydrothermal treatment

LI YUBAO

*Institute of Materials Science and Technology, Sichuan University, Chengdu 610064, Peoples Republic of China*

K. DE GROOT, J. DE WIJN, C.P.A.T. KLEIN, S.V.D. MEER

*Department of Biomaterials, University of Leiden, Rijnsburgerweg 10, bld 55, 2333 AA Leiden, The Netherlands.*

Nanograde calcium phosphate needle-like crystals are prepared from wet synthesized Ca–P precipitates by simple hydrothermal treatment at 140 °C and 0.3 MPa for 2 h. The morphology of these crystals is observed by transmission electron microscopy (TEM). The phase composition is tested through X-ray diffractometer (XRD) and infrared spectroscopy (IR). It is found that the morphology of these crystals is related to the activity or fresh degree of the starting Ca–P precipitates and the added fluorine ions, but is not greatly influenced by the Ca/P ratio of the precipitates. These crystals with a Ca/P ratio between 1.67 and 1.5 show a poorly crystallized apatite structure at room temperature and a biphasic (HA +  $\beta$  – TCP) structure at 1100 °C, corresponding to their Ca/P ratio. It is demonstrated that these nonstoichiometric apatite crystals contain lattice-bound water which could play an important role in the formation of bone apatite. The similarity in morphology and composition between these needle-like crystals and the apatite crystals in bone provides a possibility to make a bone-like implant consisting of these needle-like crystals and collagen, etc.

## 1. Introduction

Calcium phosphate is known to be the main mineral constituent of human hard tissues [1]. Sintered well-crystallized biphasic bioceramics consisting of hydroxyapatite (HA) and tricalcium phosphate (TCP), which are similar to sintered bone products [2, 3], are found to be biologically more reactive than pure HA [4, 5] and even show new bone formation in non-osseous tissues of animals [6, 7]. Nevertheless, the presence of calcium phosphate in bone is in the form of nanometre-size needle-like crystals [8–12] with a poorly crystallized nonstoichiometric apatite phase containing  $\text{CO}_3^{2-}$ ,  $\text{Na}^+$  and  $\text{F}^-$  ions, etc. [13–16].

Nonstoichiometric apatite shows a stoichiometric apatite or HA structure involving Ca and OH defects and substitution of  $\text{HPO}_4^{2-}$  groups for  $\text{PO}_4^{3-}$  ones, and possesses a Ca/P ratio between 1.67 and 1.33 [17]. Its accepted formula is  $\text{Ca}_{10-x}(\text{HPO}_4)_x(\text{PO}_4)_{6-x}(\text{OH})_{2-x}$  ( $0 < x < 2$ ) [18]. The Ca/P ratio of bone apatite is generally between 1.67 and 1.50 [2, 3], corresponding to  $0 < x < 1$ . In order to build a bone-like composite composed of collagen and bone-apatite-like crystals for bone repair and replacement, it is necessary to study and prepare nanometre-size nonstoichiometric apatite needle-like crystals. In this paper, a simple hydrothermal processing is employed to make such bone-apatite-like crystals.

## 2. Materials and methods

Analytical grade reagents  $(\text{NH}_4)_2\text{HPO}_4$  and  $\text{Ca}(\text{NO}_3)_2$  were used to synthesize starting Ca–P precipitates, according to a method similar to Jarcho *et al.* [19]. The  $(\text{NH}_4)_2\text{HPO}_4$  aqueous solution was slowly dropped into the stirred  $\text{Ca}(\text{NO}_3)_2$  aqueous solution. The pH for both solutions was 10 to 12, adjusted with ammonium solution, and the reaction was carried out at room temperature (RT). The as-prepared precipitates were put into an autoclave in a solid–solution ratio of 1 wt % and hydrothermally treated at 140 °C and 0.3 MPa for 2 h, after centrifugal washing with deionized water. In order to study the influence of the fluorine ion on the crystal growth, 0.1 wt % NaF, relative to the total weight of the  $(\text{NH}_4)_2\text{HPO}_4$  and  $\text{Ca}(\text{NO}_3)_2$  used, was added to the  $(\text{NH}_4)_2\text{HPO}_4$  solution before synthesization. The same precipitation and hydrothermal condition was kept for  $\text{F}^-$ -containing precipitates.

The Ca/P ratio of those hydrothermally treated samples was measured with an atomic absorption spectrometer for calcium and an ultraviolet spectrophotometer for phosphorus. The morphology was observed by transmission electron microscopy (TEM). The phase was observed by transmission electron microscopy (TEM). The phase composition was tested through X-ray diffractometry (XRD) and infrared spectroscopy (IR).

### 3. Results

#### 3.1. TEM photographs

The morphology of the hydrothermally formed needle-like crystals are shown in Fig. 1a (sample N-1) and Fig. 1b (sample N-2), and are for samples with a Ca/P ratio of 1.59 and 1.52, respectively, without the addition of  $F^-$  ions. The shape and size of sample N-1 and N-2 are basically the same. Fig. 1c (sample N-3) is for  $F^-$ -containing crystals with a Ca/P ratio of 1.61. These  $F^-$  ions are 1.38 wt% measured by fluorene ionic electrode. These  $F^-$ -containing, needle-like crystals look much thinner than those in Fig. 1a and b. The mean crystal size for sample N-2 and sample N-3 is about 23 nm by 91 nm and 10 nm by 75 nm, respectively, according to measurement of the length and width of these crystals under microscope. It has been noticed that when heating at 600–650 °C, these samples show a decrease in crystal length or volume. Fig. 1d shows the morphology of sample N-2 after heating at 650 °C; the calculated mean crystal size is about 22 nm by 67 nm using the same measurement method mentioned above. The data for mean crystal size of sample N-2 before and after heating at 650 °C shows a 35% decrease in the average crystal volume.

#### 3.2. XRD patterns

All the three samples give a similar poorly crystallized apatite or HA structure, as shown in Fig. 2a. This

indicates that these samples with a Ca/P ratio between 1.67 and 1.50 are poorly crystallized, nonstoichiometric apatite crystals. When heated to different temperatures, these samples show a similar apatite structure to that in Fig. 2a below 650 °C and a biphasic (HA +  $\beta$ -TCP) structure above 650 °C. The TCP content increases with increasing temperature and reaches its final value at 1100 °C. Fig. 2b shows the XRD pattern of sample N-2 after heating at 650 °C. A trace amount of TCP phase can be observed. The 1100 °C XRD patterns for samples N-1, N-2 and N-3 are shown in Fig. 2c, d and e, respectively, in which the relative content of HA and TCP phase is consistent with their respective Ca/P ratio.

#### 3.3. IR spectra

The IR spectra of the three samples are shown in Fig. 3a–c, which indicate the presence of  $OH^-$ ,  $H_2O$ ,  $HPO_4^{2-}$  and  $PO_4^{3-}$  as well as  $CO_3^{2-}$ . The peaks at 3571 and 633  $cm^{-1}$  are due to  $OH^-$  ions, the 875  $cm^{-1}$  peak is caused by  $HPO_4^{2-}$  ions. The broad bands from 3700 to 2500  $cm^{-1}$  and around 1635  $cm^{-1}$  arise from water, the 1456 and 1426  $cm^{-1}$  peaks are from  $CO_3^{2-}$  ions. The shoulder at about 585  $cm^{-1}$  and the broad band from 800 to 650  $cm^{-1}$  in Fig. 3c are related to  $F^-$  ions. Other peaks are due to  $PO_4^{3-}$  ions. It can be seen that the  $CO_3^{2-}$  content in samples N-1

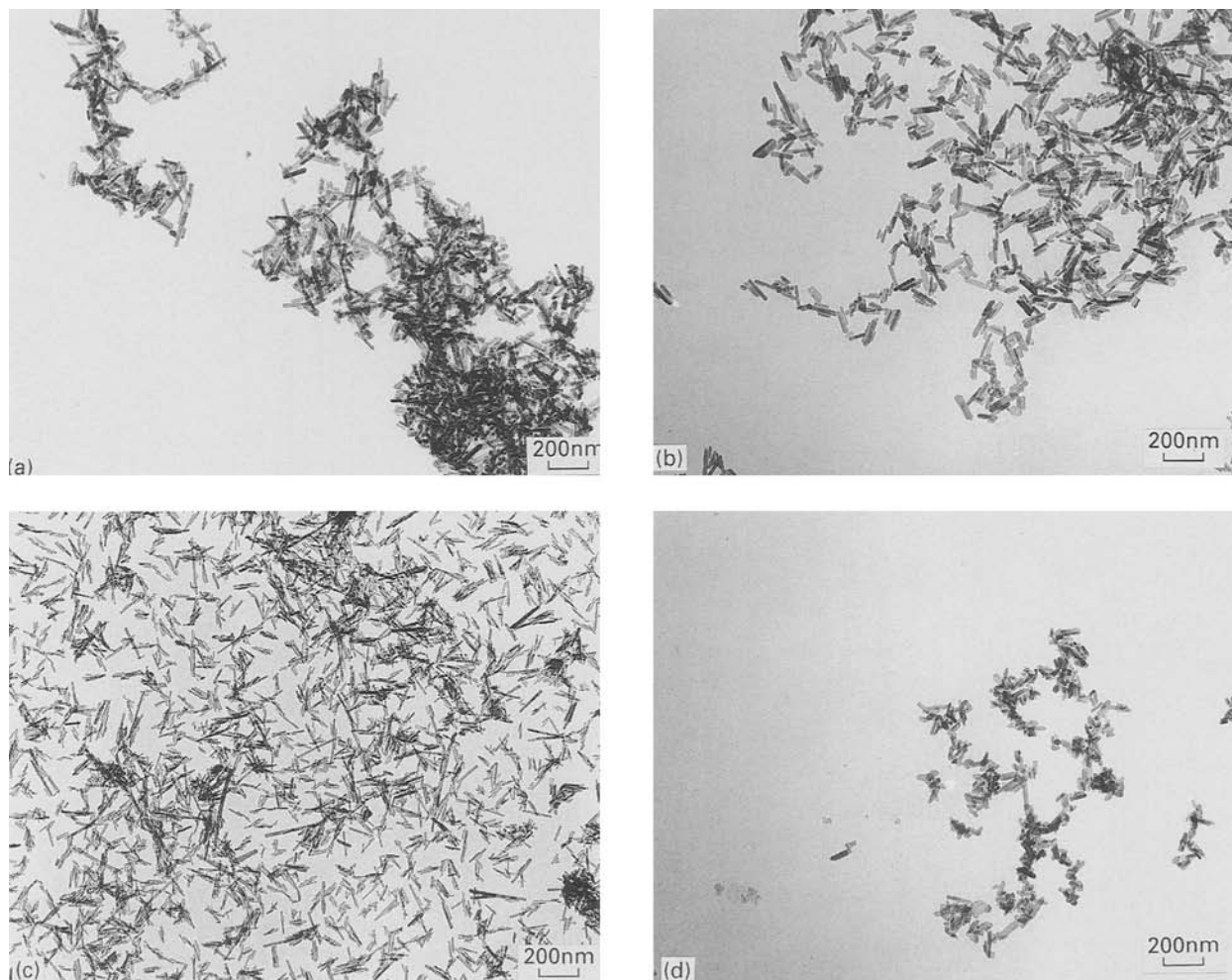


Figure 1 TEM photographs of the needle-like crystals: (a) sample N-1; (b) sample N-2; (c) sample N-3; (d) sample N-2 heated to 650 °C.

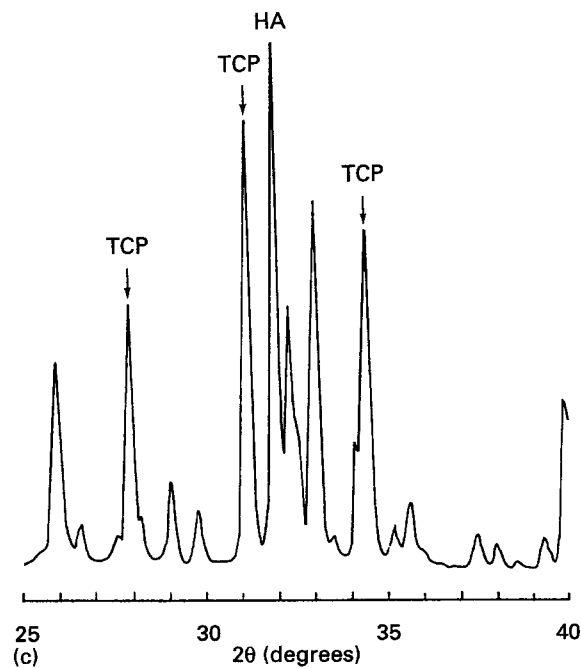
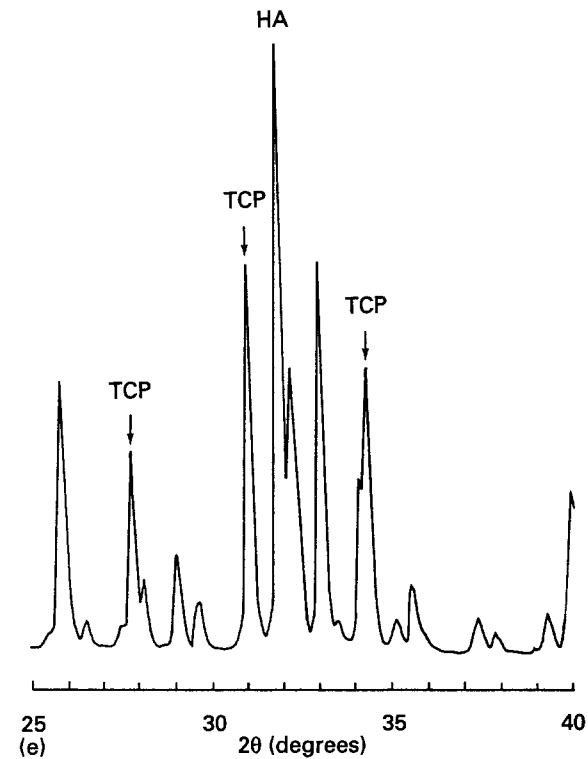
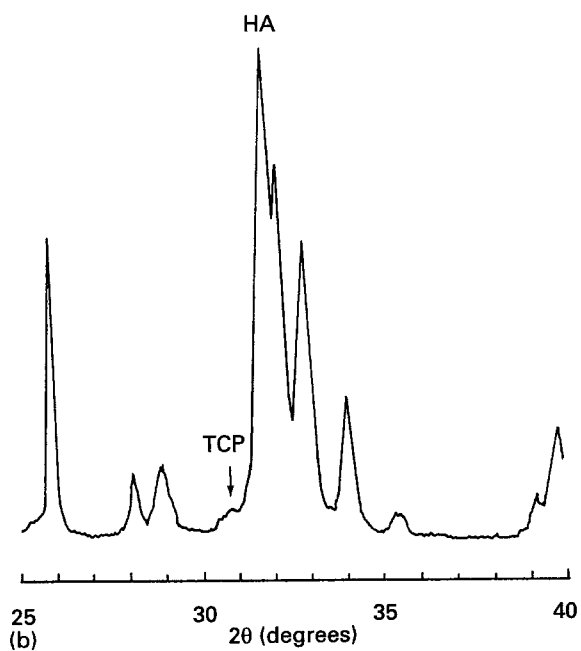
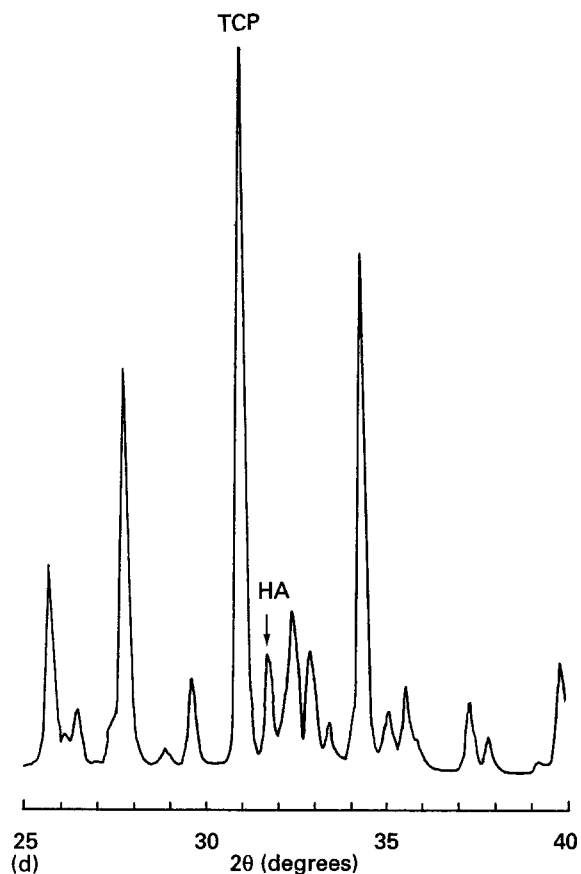
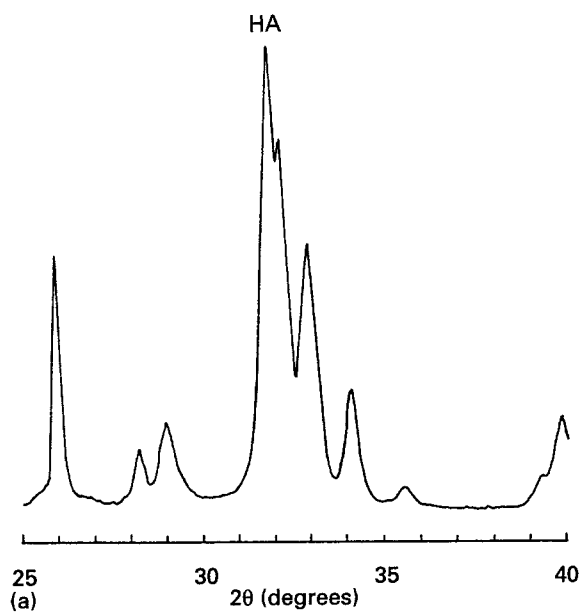


Figure 2 XRD patterns of the needle-like crystals: (a) poorly crystallized apatite (HA) structure (b) sample N-2 heated to 650 °C; (c) sample N-1 heated to 1100 °C; (d) sample N-2 heated to 1100 °C; (e) sample N-3 heated to 1100 °C.

and N-2 is very small and increases significantly when  $F^-$  ions are contained in the nonstoichiometric apatite crystals. Fig. 3c shows only a shoulder for the  $OH^-$  peak at  $3571\text{ cm}^{-1}$ , the  $633\text{ cm}^{-1}$   $OH^-$  peak is absent. Fig. 3d shows the IR spectrum for sample N-2

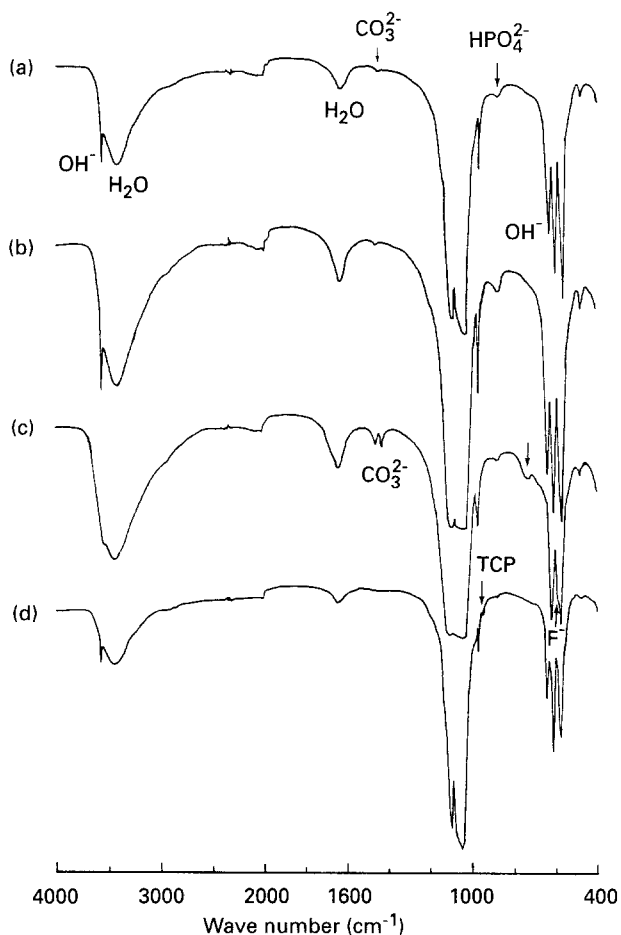


Figure 3 IR spectra of the needle-like crystals (a) sample N-1; (b) sample N-2; (c) sample N-3; (d) sample N-2 heated to 750 °C.

after heating at 750 °C. The peak at 940  $\text{cm}^{-1}$  is from the  $\beta$ -TCP phase. The water and  $\text{OH}^-$  peaks decrease noticeably and the  $\text{CO}_3^{2-}$  peak completely disappears, but the 875  $\text{cm}^{-1}$   $\text{HPO}_4^{2-}$  peak is still present.

#### 4. Discussion

It can be noted that samples N-1 and N-2 bear some resemblance in morphology and size, although their Ca/P ratios are different. The mean crystal size of sample N-2 is about 23 nm by 91 nm, which is very close to the mean size 23.7 nm by 90 nm (aspect ratio = 3.8) given by Ioko *et al.* [20], who prepared needle-like pure HA (Ca/P = 1.67) crystals with the mean size mentioned above by a similar hydrothermal method at 200 °C and 2 MPa for 10 h. This means that the Ca/P ratio of the precipitates, and the difference between the hydrothermal conditions used by Ioko and this experiment have not shown an appreciable influence on the morphology of these needle-like crystals, in spite of the fact that the crystallinity of these crystals improves with an increase in hydrothermal pressure or temperature [20]. However, short crystals were obtained if Ca–P precipitates synthesized at 70 °C, or 5-day standing Ca–P precipitates were used in the hydrothermal treatment, as shown in Fig. 4. This indicates that the activity or “freshness” of the precipitates is an important factor in addition to the

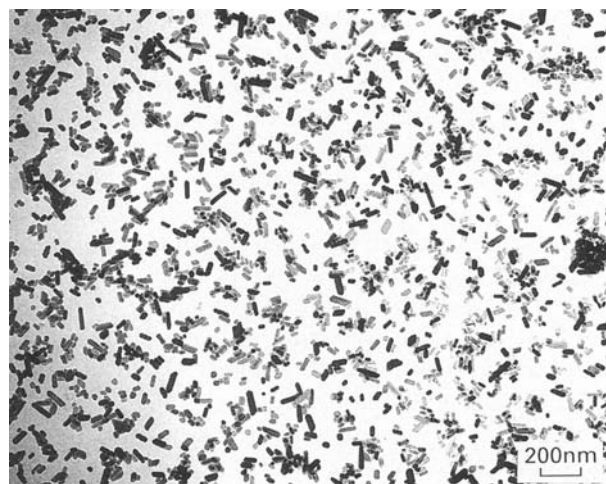


Figure 4 TEM photograph of the short needle-like crystals.

$\text{F}^-$  ions that affects the morphology of the needle-like crystals. The relatively high temperature (70 °C) or long standing time renders the precipitates less active than the as-prepared precipitates at RT.

It is clear that the activity of the precipitates primarily influences the length of the needle-like crystals while the  $\text{F}^-$  ions influence not only the length, but also the width. The disappearance of the 633  $\text{cm}^{-1}$  peak in Fig. 3c is caused by the  $\text{F}^-$  ions situated in the  $\text{OH}^-$  sites. But the shoulder at 3571  $\text{cm}^{-1}$  still indicates the presence of  $\text{OH}^-$  ions in the  $\text{F}^-$ -containing apatite crystal structure. The existence of the  $\text{CO}_3^{2-}$  ions in the  $\text{F}^-$ -containing crystals could come from the coupling of the  $\text{Na}^+$  from NaF with  $\text{CO}_2$  or  $\text{CO}_3^{2-}$  in water. The carbonate incorporation is thus possibly by the substitution of  $\text{Na}^+ + \text{CO}_3^{2-}$  for  $\text{Ca}^{2+} + \text{PO}_4^{3-}$ , and both the  $\text{F}^-$  ions and the  $\text{CO}_3^{2-}$  ions have an influence on the apatite crystallite size [21]. Therefore, the thin  $\text{F}^-$ -containing needle-like crystals should be the outcome of the common action of  $\text{F}^-$  and  $\text{CO}_3^{2-}$  ions. After remaining in distilled water for 5 months, sample N-2 shows no change, in both morphology and composition. This means that distilled water can be chosen to preserve these crystals until required for use in a solution or slurry state. To date, there has been no method able to dry such nanometre-size apatite crystals without agglomeration.

After heating at 650 °C, the decrease in the mean crystal size or average volume of sample N-2 should be attributable to the release of water. The water could be from the condensation of  $\text{HPO}_4^{2-}$  ions or from lattice-bound ions. It is known that the  $\text{HPO}_4^{2-}$  ion in  $\text{CaHPO}_4 \cdot 2\text{H}_2\text{O}$  turns completely into  $\text{P}_2\text{O}_7^{4-}$  ion when heated to 600 °C [2, 18], at the same time giving out water according to the reaction:  $2\text{HPO}_4^{2-} \rightarrow \text{P}_2\text{O}_7^{4-} + \text{H}_2\text{O}$ . But, in the 750 °C IR spectrum in Fig. 3d, the  $\text{HPO}_4^{2-}$  peak can clearly be seen. The same phenomena were also found by other authors at similar temperature ranges [22–24]. This means that the condensation of  $\text{HPO}_4^{2-}$  ions in non-stoichiometric apatite crystals is different from, or more difficult, than that in  $\text{CaHPO}_4 \cdot 2\text{H}_2\text{O}$  materials, due to the small quantity of the  $\text{HPO}_4^{2-}$  ions in, or to

the restriction from, the nonstoichiometric apatite crystal structure. On the other hand, when heating above 650 °C, the nonstoichiometric apatite crystals become a biphasic HA +  $\beta$ -TCP structure, in which  $\beta$ -TCP phase increases with increasing temperature, while the residual HA phase decreases with increasing temperature. It is possible that the residual HA phase could still be a nonstoichiometric apatite. For sample N-2 (Ca/P ratio = 1.52), when a part of  $\beta$ -TCP phase with the lowest Ca/P ratio 1.50 is formed at 750 °C, the residual HA phase containing  $\text{HPO}_4^{2-}$  ions (Fig. 3d) will have a Ca/P ratio more than 1.52 but less than 1.67, because the total Ca/P ratio 1.52 is a constant. Thus, the  $\beta$ -TCP phase formed above 650 °C should be the result of the two successively occurring reactions; the condensation of the  $\text{HPO}_4^{2-}$  ions ( $2\text{HPO}_4^{2-} \rightarrow \text{P}_2\text{O}_7^{4-} + \text{H}_2\text{O}$ ) and the reaction of  $\text{P}_2\text{O}_7^{4-}$  with  $\text{OH}^-$  ions ( $\text{P}_2\text{O}_7^{4-} + 2\text{OH}^- \rightarrow 2\text{PO}_4^{3-} + \text{H}_2\text{O}$ ). Sufficient  $\text{OH}^-$  ions adjacent to the newly formed  $\text{P}_2\text{O}_7^{4-}$  ions in the nonstoichiometric apatite crystal structure ensure that the second reaction happens readily and rapidly. Therefore the trace TCP phase in the 650 °C XRD pattern indicates that only a small amount of  $\text{HPO}_4^{2-}$  ions are condensed at this moment. As a result of this, the near-35% decrease in the average crystal volume of sample N-2 can be ascribed primarily to the release of lattice-bound water.

The presence of the lattice-bound water in nonstoichiometric apatite crystals indicates that water could play a role in the formation of bone apatite. This is important for the further understanding of the mechanism of calcified tissues and bone-bonding phenomenon of calcium phosphate biomaterials. The formation process of the Ca-P precipitates into these small needle-like nonstoichiometric apatite crystals in the hydrothermal environment may be comparable with that of the Ca-P precursor into the bone apatite of the developing fetus in the maternal abdominal cavity. Both processes happen at a certain temperature, under certain pressure and in a closed system containing water, although the latter process is much more complicated.

As we know, the mineral of natural bone is chiefly composed of nonstoichiometric apatite crystals which contain a certain amount of  $\text{CO}_3^{2-}$ ,  $\text{Na}^+$  and  $\text{F}^-$  ions, etc. Bone apatite crystals are found to be needle-like crystals with a size of 5–20 nm by 60 nm [8] or 3 nm by 40 nm [25], while the crystallites in dental enamel contain more  $\text{F}^-$  ions than bone [21] and grow much longer, over 100 nm in length [8]. The different data and size are probably related to both the  $\text{F}^-$  ions and the  $\text{CO}_3^{2-}$  ions they contain, in addition to other factors, such as species and sites. Sample N-1 and N-2 show only a very small  $\text{CO}_3^{2-}$  peak in their IR spectra. In order to increase the  $\text{CO}_3^{2-}$  in these samples, a method that incorporates carbonate in the apatite structure by soaking apatite crystals in mineral or carbonated water can be utilized [26]. In fact, when these nonstoichiometric apatite crystals are implanted in a living body, the body fluid may also result in such an effect.

In brief, the hydrothermal treatment used in this

experiment is a simple, practical and reproducible method to prepare nanometre-size needle-like crystals. The similarity in morphology and composition of the hydrothermally formed nonstoichiometric apatite needle-like crystals and the apatite crystals in bone might lead to an improvement of osteointegration in bony sites. It enables scientists to make composite implants comparable to bone, in which the nanograde needle-like crystals are embedded or inserted and chemically and biologically linked via a collagenic structure. It is also helpful in promoting further understanding of the nature and properties of calcified tissues.

## Acknowledgements

The authors thank Mr Joop Wolke, Mrs Jolanda de Blicck and Mr Jurren Koerts for their assistance with the experiments. They are also grateful to the Commission of the European Communities for subsidizing this study.

## References

1. K. DE GROOT, "Bioceramics of calcium phosphate" (CRC Press, Boca Raton, 1983).
2. A. HIRSCHMAN, A. E. SOBEL, B. KRAMER and I. FANKUCHEN, *J. Biol. Chem.* **171** (1947) 285.
3. R. M. BILTZ and E. D. PELLEGRINO, *J. Dent. Res.* **62** (1983) 1190.
4. P. FRAYSSINET, J. L. TROUILLET, N. ROUQUET, E. AZIMUS and A. AUTEFAGE, *Biomaterials* **14** (1993) 423.
5. G. DACULSI, N. PASSUTI, S. MARTIN, C. DEUDON, R. Z. LEGEROS, and S. RAHER, *J. Biomed. Mater. Res.* **24** (1990) 379.
6. LI YUBAO, ZHANG XINGDONG, CHEN WEIQUN, LIU YUHUA, C. P. A. T. KLEIN and K. DE GROOT, in Transactions of the 19th Annual Meeting of Society For Biomaterials, Birmingham, April, 1993 (Society For Biomaterials, Minneapolis, USA, 1993) p. 165.
7. C. P. A. T. KLEIN, K. DE GROOT, CHEN WEIQUN, LI YUBAO and ZHANG XINGDONG, *Biomaterials* **15** (1994) 31.
8. J. L. KATZ and R. A. HARPER, in "Encyclopedia of materials science and engineering" (Pergamon, Oxford, 1986) p. 475.
9. A. ENGSTROM, *Exp. Cell Res.* **43** (1966) 241.
10. J. D. TERMINE, E. D. EANES, D. J. GREENFIELD, M. U. NYLEN and R. A. HARPER, *Calcif. Tissue Res.* **12** (1974) 73.
11. W. J. LANDIS, M. C. PAINE and M. J. GLIMCHER, *J. Ultrastruct. Res.* **59** (1977) 1.
12. A. ASCENZI, A. BIGI, M. H. KOCK, A. RIPAMONTI and A. ROVERI, *Calcif. Tissue Int.* **37** (1985) 659.
13. A. S. POSNER, in "Bone and mineral research", Vol. 5, edited by W. A. Peck (Elsevier, Amsterdam, 1987) p. 65.
14. E. D. EANES, in "Bone regulatory factors", edited by A. Pecile and B. de Bernard, NATO ASI Series (Plenum Press, New York, 1990) p. 1.
15. G. MONTEL, G. BONEL, J. C. HEUGHEBAERT, J. C. TROMBE and C. REY, *J. Cryst. Growth* **53** (1981) 74.
16. P. DUCHEYNE, *J. Biomed. Mater. Res.* **21** (A2) (1987) 219.
17. A. MORTIER, J. LEMAITRE, L. RODRIQUE and P. G. ROUXHET, *J. Solid State Chem.* **78** (1989) 215.
18. J. L. LACOUT, in "Biomaterials-hard tissue repair and replacement", edited by D. Muster (Elsevier Science Publishers, B. V., Amsterdam 1992) p. 81.
19. M. JARCHO, C. H. BOLEN, M. B. THOMAS, J. BOBICK, J. F. KAY and R. H. DOREMUS, *J. Mater. Sci.* **11** (1976) 2027.
20. K. IOKU and M. YOSHIMURA, *Phosphorus Res. Bull.* **1** (1991) 15.

21. R. Z. LEGEROS and M. S. TUNG, *Caries Res.* **17** (1983) 419.
22. J. ARENDS, J. CHRISTOFFERSEN, M. R. CHRISTOFFERSEN, H. ECKERT, B. O. FOWLER, J. C. HEUGHEBAERT, G. H. NANCOLLAS, J. P. YESINOWSKI and S. J. ZAWACKI, *J. Cryst. Growth* **84** (1987) 515.
23. E. E. BERRY, *J. Inorg. Nucl. Chem.* **29** (1967) 317.
24. JIMING ZHOU, XINGDONG ZHANG, JIYONG CHEN, SHAOXIAN ZENG and K. DE GROOT, *J. Mater. Sci. Mater. Med.* **4** (1993) 83.
25. J. B. PARK and R. S. LAKES, in "Biomaterials: an introduction" (Plenum Press, New York and London, 1992) p. 192.
26. E. G. NORDSTROM and K. H. KARLSSON, *J. Mater. Sci.: Mater. Med.* **1** (1990) 182.